Blue Light Activates Phase 2 Response Proteins and Slows Growth of A431 Epidermoid Carcinoma Xenografts

ALPESH D. PATEL[1,2], SHAUN ROTENBERG[1,3], REGINA L.W. MESSER[1], JOHN C. WATAHA[1,4], KALU U.E. OGBUREKE[1,5], VERONICA V. MCCLOUD[1], PETRA LOCKWOOD[1], STEPHEN HSU[1] and JILL B. LEWIS[1,6]

[1]Department of Oral Biology, Georgia Regents University, Augusta, GA, U.S.A.; Divisions of [2]Orthodontics, and [3]Periodontics, The Ohio State University, Columbus, OH, U.S.A.; [4]Department of Restorative Dentistry, University of Washington, Seattle, WA, U.S.A.; [5]Department of Diagnostic and Biomedical Sciences, University of Texas School of Dentistry at Houston, Houston, TX, U.S.A.; [6]College of Dental Medicine, Western University of Health Sciences, Pomona, CA, U.S.A.

Abstract. *Background: Recent studies suggest that light in the UVA range (320-400 nm) activates signaling pathways that are anti-inflammatory, antioxidative and play a critical role in protection against cancer. These effects have been attributed to NF-E2-related factor (NRF2)-mediated up-regulation of 'phase 2' genes that neutralize oxidative stress and metabolize electrophiles. We had previously shown that small doses of blue light (400-500 nm) had selective toxicity for cultured oral tumor cells and increased levels of peroxiredoxin phase 2 proteins, which led to our hypothesis that blue light activates NRF2 signaling. Materials and Methods: A431 epidermoid carcinoma cells were treated in culture and as nude mouse xenografts with doses of blue light. Cell lysates and tumor samples were tested for NRF2 activation, and for markers of proliferation and oxidative stress. Results: Blue light activated the phase 2 response in cultured A431 cells and reduced their viability dose dependently. Light treatment of tumors reduced tumor growth, and levels of proliferating cell nuclear antigen (PCNA), and oxidized proteins. Discussion: Cellular responses to these light energies are worth further study and may provide therapeutic interventions for inflammation and cancer.*

With wavelengths of 400-500 nm, visible blue light energy has been used extensively in dentistry to activate polymerization of adhesives and resin composites, with no documented adverse patient effects. However, the effect of exposure to blue light on cells and tissues is less well-defined. Until recently, most research has characterized blue light–tissue interactions from the stand-point of biological safety, particularly in the skin and retina, where blue light-induced reactive oxygen species (ROS) are suspected mediators of skin aging and age-related macular degeneration (1-3). Several studies have reported that blue light disrupts cellular processes such as mitosis, mitochondrial function, and DNA integrity, and that light-induced ROS probably mediate these effects as well (3-5). More recent studies have begun to examine cell signaling pathways that are modulated by light energy. Again, most of them have focused on UV wavelengths, but some have looked at energies in the visible light range. Many of these studies suggest that light in the UVA range (320-400 nm) may activate cytoprotective pathways that are both anti-inflammatory and antioxidative (6), and which play a critical role in protection against cancer. These effects are thought to be mediated through activation of the redox-sensitive transcription factor, NF-E2-related factor (NRF2), and subsequent up-regulation of genes that serve to help neutralize oxidative stress and metabolize electrophiles.

NRF2 is a stress-responsive transcription factor that, under normal conditions, is kept sequestered in the cytoplasm by an inhibitor protein called Kelch-like ECH-associated protein 1 (KEAP1) (7-10). When bound to KEAP1, a multi-lysine-containing alpha helix of NRF2 is available that may serve to receive ubiquitin and thus target NRF2 for proteosomal degradation (11). Therefore, much like p53, NRF2 is constantly synthesized and degraded but can accumulate rapidly to respond to stress conditions. One way that the stress response is thought to be activated is *via* reactive cysteine residues on both NRF2 and KEAP1 that can respond to oxidative stress by

Correspondence to: Jill B. Lewis, College of Dental Medicine, Western University of Health Sciences, 309 East Second Street, Pomona, CA 91766-1854, U.S.A. Tel: +1 9094698257, Fax: +1 9097063800, e-mail: lewisj@westernu.edu

Key Words: NRF2, heme oxygenase, xenograft, oxidative stress, blue light.

forming disulfides, resulting in major conformational shifts that ultimately lead to NRF2 release and translocation to the nucleus (12). Once in the nucleus, NRF2 complexes with small musculoaponeurotic fibrosarcoma proteins and binds to enhancer sequences called antioxidant response elements that activate transcription of sets of genes whose products help to neutralize ROS and metabolize xenobiotics (10, 13). These genes, often called the phase 2 response genes, include the enzymes for synthesis of glutathione, the peroxiredoxins, and heme oxygenase 1 (HO1) (14, 15).

Evidence is mounting for a role of the phase 2 proteins in governing inflammation, with an overlapping influence on tumorigenesis. *Nrf2*-knockout mice have exaggerated responses to inflammatory challenge (16, 17), and, in some tumorigenesis models, also generate more tumors in response to tumor initiator/promoter treatment (18, 19). NRF2 is activated by many phytochemicals, and this activation has been shown to reduce inflammation and tumor cell growth in many studies (18, 20-22). Most likely this effect is due to cross-talk between NRF2 transcriptional regulation and nuclear factor-kappa B (NF-κB), a major pro-inflammatory transcription factor (21, 23). Up-regulation of *NRF2* and *HO1* results in down-regulation of many pro-inflammatory cytokines and enzymes that are regulated by NF-κB (24, 25). In addition, constitutive NF-κB activation is often associated with tumors because it also regulates production of several pro-proliferative and anti-apoptotic proteins. Therefore, the NRF2-mediated phase 2 response is becoming a popular target for therapeutic interventions that can simultaneously up-regulate the phase 2 proteins and down-regulate NF-κB-mediated signaling.

Our laboratory previously showed that small, discreet doses of blue-violet light (380-500 nm) delivered from a quartz-tungsten-halogen (QTH) dental curing light source has selective toxicity for cultured oral tumor cells, with no apparent toxicity for normal keratinocytes (26). No pre-loaded photoactivator compound is used as in photodynamic therapy, so this toxicity is a result of light treatment alone. Our previous studies showed that blue light treatment induced generation of ROS and enhanced apoptosis of oral tumor cells in culture, and proteomics analysis revealed significantly increased levels of peroxiredoxins in THP-1 monocytic cells in response to blue light exposure (26). Together, these results led us to the present study in which we examined whether blue light exposure activated NRF2 and induced phase 2 responses in an epidermoid tumor cell line, A431, and whether light treatment of A431 tumor xenografts had a therapeutic effect in a nude mouse model.

Materials and Methods

Cell culture. The human epidermoid carcinoma cell line A431 was chosen because of its propensity to produce tumors in nude mice without metastasis. A431 cells were purchased from the American Type Culture Collection (Manassas, VA, USA) and cultured according to their recommendations in Dulbecco's modified Eagle's medium (DMEM, Sigma, St. Louis, MO, USA) supplemented with 10% fetal bovine serum, 100 U/ml penicillin and 100 μg/ml streptomycin. Cells were cultured in a humidified, 5% CO_2 atmosphere at 37˚C.

Blue light exposure. Blue light was delivered from a QTH dental curing light (500 mW/cm^2; VIP, Bisco, Schaumburg, IL, USA). This light source is manufactured to deliver defined intraoral doses of light with a 400-500 nm spectral output without significant UV or infrared components (see Figure 1), at uniform energy densities. Fiberoptic tips (6.4 mm and 15.6 mm diameter) were used to uniformly treat cell cultures in a 96- or 24-well format, respectively, at a distance of 7.5 mm from the medium surface. Light units were calibrated prior to each experiment using a Demetron radiometer (Kerr Corp., Orange, CA, USA).

Mice. Female *nu/nu* athymic mice (4-6 weeks old) were purchased from the National Cancer Institute (Bethesda, MD, USA), housed under sterile conditions and treated in accordance to Georgia Regents University Institutional Animal Care and Use Committee established guidelines, protocol approval number 06-05-819.

Nude mouse xenografts. Cultured A431 human epidermoid carcinoma cells were injected subcutaneously at a density of 1.5×10^6 cells/100 μl sterile PBS into the abdomens of female *nu/nu* athymic mice (n=10) and xenograft growth was monitored daily. At day 12, mice were divided randomly into control and light-treated groups (five mice each). Tumors from the light-treated animals were exposed daily to 45 J/cm^2 (90 sec) doses of blue light delivered from a QTH dental light curing unit. Tumor volumes were assessed at days 1, 3, 5, 8, and 12 post-light treatment by caliper measurement. The tumor volume was calculated as the width^2×length/2 (mm^3). Tumors were harvested at day 23. Each tumor was divided into equal parts that were flash-frozen or fixed in 10% neutral-buffered formalin. Flash-frozen tumors were ground in liquid nitrogen and homogenized in lysis buffer (1% SDS, 1.0 mM sodium orthovanadate, 10 mM Tris-HCl, pH 7.4, and 2 mM EDTA). Fixed tumors were embedded in paraffin and sectioned at 5 μm.

MTT assay. To determine mitochondrial activity/cellular viability of light-treated A431 cells, succinate dehydrogenase (SDH) activity was measured *via* the 3-(4,5-dimethylthiazol-2-yl)-2,5-diphenyltetrazolium bromide (MTT) method. A431 cell samples were treated with 0, 15 or 45 J/cm^2 doses of light from a QTH dental light curing unit and were incubated for 24, 48 or 72 h. At the appropriate time point, 2% MTT solution in 0.25 M sodium succinate was added and formazan crystal formation was allowed to proceed for 1 hour. Cells were then formalin fixed and solubilized in dimethylsulfoxide, and formazan production was quantified by absorbance spectroscopy at 562 nm. The SDH activity was expressed as a percentage of untreated controls.

Cell fractionation. Cytosolic and nuclear fractions were prepared as described previously (27). Briefly, control and blue light-treated A431 cells were washed with phosphate buffered saline (PBS) to remove media components, resuspended in hypotonic lysing buffer and left on ice for 15 min to lyse the cells. Nuclei were pelleted by centrifugation and the cytosolic fraction (supernatant) was removed,

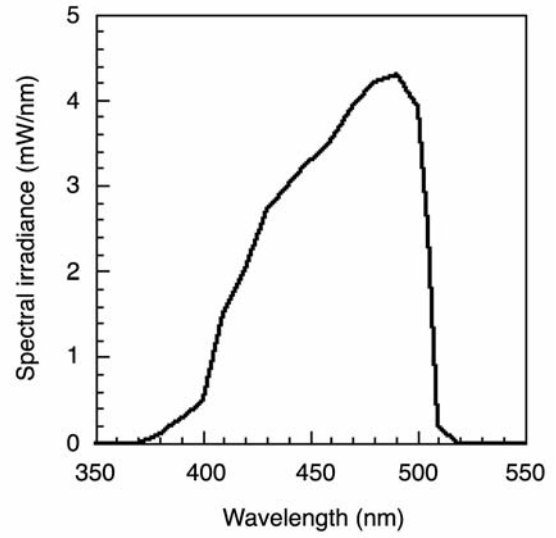

Figure 1. *Spectral output of quartz-tungsten-halogen curing lights used in this study (VIP, Bisco).*

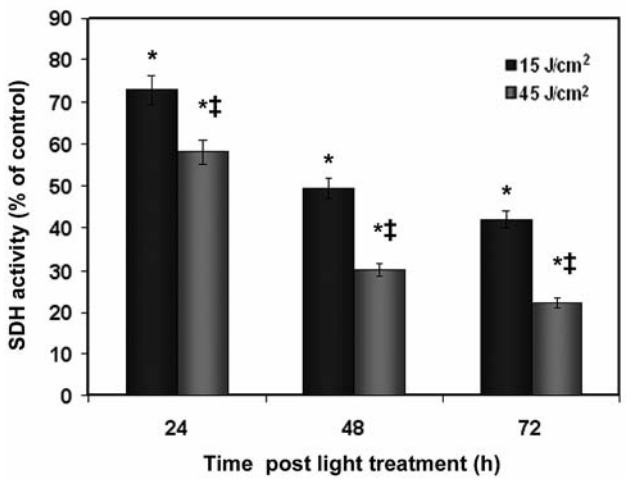

Figure 2. *3-(4,5-dimethylthiazol-2-yl)-2,5-diphenyltetrazolium bromide (MTT) assay: Cellular viability estimated by mitochondrial succinate dehydrogenase activity (MTT method), displayed as the percentage of untreated controls (set at 100%) at 24, 48, and 72 h post-light treatment (15 J/cm^2 and 45 J/cm^2 doses). Error bars indicate 1 standard deviation (n=3). *Significantly different from the control (ANOVA, Tukey post-hoc pair-wise comparison tests, α=0.05); ‡significant difference between doses at each time point (two-sided Student's t-test, p<0.05).*

diluted with an equal volume of 2× Laemmli's sample buffer, flash frozen and stored at −80˚C. The nuclear fraction was resuspended in hypertonic buffer, left on ice for 30 min, then nuclear membranes were pelleted by centrifugation at 16000 × *g* for 30 min. Supernatant containing nuclear proteins was removed, diluted with an equal volume of 2× Laemmli's sample buffer, flash frozen and stored at −80˚C. All samples were boiled for 3 min prior to sodium dodecyl sulfate-polyacrylamide gel electrophoresis (SDS-PAGE).

Western blot analysis. Western blot analysis was performed on nuclear and cytosolic protein lysates prepared from A431 cells grown in 24 well plates, exposed to 0, 15, or 45 J/cm^2 of blue light and harvested at 0.5, 1, 2, and 6 h post-light treatment. Additional analyses were performed on tumor samples from flash-frozen A431 xenografts. Proteins were separated by 9% SDS-polyacrylamide gel electrophoresis, transferred to polyvinylidene fluoride (PVDF) membranes (Immobilon, EMD Millipore, Billerica, MA, USA) by semi-dry electrophoretic transfer, and exposed to antibodies specific for NRF2, NF-κB, and proliferating cell nuclear antigen (PCNA; tumor samples only) (all from Santa Cruz Biologicals, Santa Cruz, CA, USA), or HO1 (Enzo Life Sciences, Farmingdale, NY, USA). β-Actin (Santa Cruz Biologicals) staining was used as a loading control.

Protein lysates prepared from flash-frozen tissues were used in western blot procedures to assess cell proliferation (PCNA levels) and generalized protein oxidation (OxyBlot Protein Oxidation Kit; Chemicon International, Temecula, CA, USA) of 2,4-dinitrophenylhydrazine (DNPH)-derivatized carbonyl groups. Oxidized protein profiles were derived from tumor samples derivatized with the DNPH compound, then separated by 12% SDS-PAGE and transferred to PVDF membranes. The proteins were probed with antibody to DNPH, and scanned with an Odyssey infrared scanner (LI-COR Biosciences, Lincoln, NE, USA). Five major oxidized proteins were selected and quantified in each sample. These values were then averaged in control and light-treated samples. Protein–antibody complexes were identified using Odyssey imaging analysis (LI-COR).

Statistics. Where two conditions were compared, differences between groups were assessed using two-tailed Student's *t*-tests, with p<0.05 as the limit of significance. Where multiple groups were compared, one-way ANOVA was used to determine significant differences, with Tukey pair-wise *post-hoc* analyses used to identify specific differences between pairs (α=0.05).

Results

Assessment of mitochondrial function. MTT assay results indicated that blue light treatment reduced the viability of A431 epidermoid carcinoma cells in a significant and dose-dependent manner (Figure 2). Our modified MTT assay procedure treated the cells in a buffer containing only succinate as an energy source. Therefore, this procedure was considered to primarily measure SDH activity and is thus an indirect measure of mitochondrial function. Mitochondrial activity was reduced by low-dose exposure (15 J/cm^2) by ~25% at 24 h and >50% by 72 h. Higher dose exposure (45 J/cm^2) was even more effective, reducing mitochondrial activity by >40% at 24 h and progressing to nearly an 80% reduction by 72 h.

Quantification and cellular localization of phase 2 proteins. Treatment of A431 cells with 15 and 45 J/cm^2 doses of blue light resulted in dose-dependent changes in phase 2 protein levels and cellular localization as measured by western blot analysis of cytosolic and nuclear fractions harvested at 30 min, 1, 2, and 6 hours post-light treatment. A representative

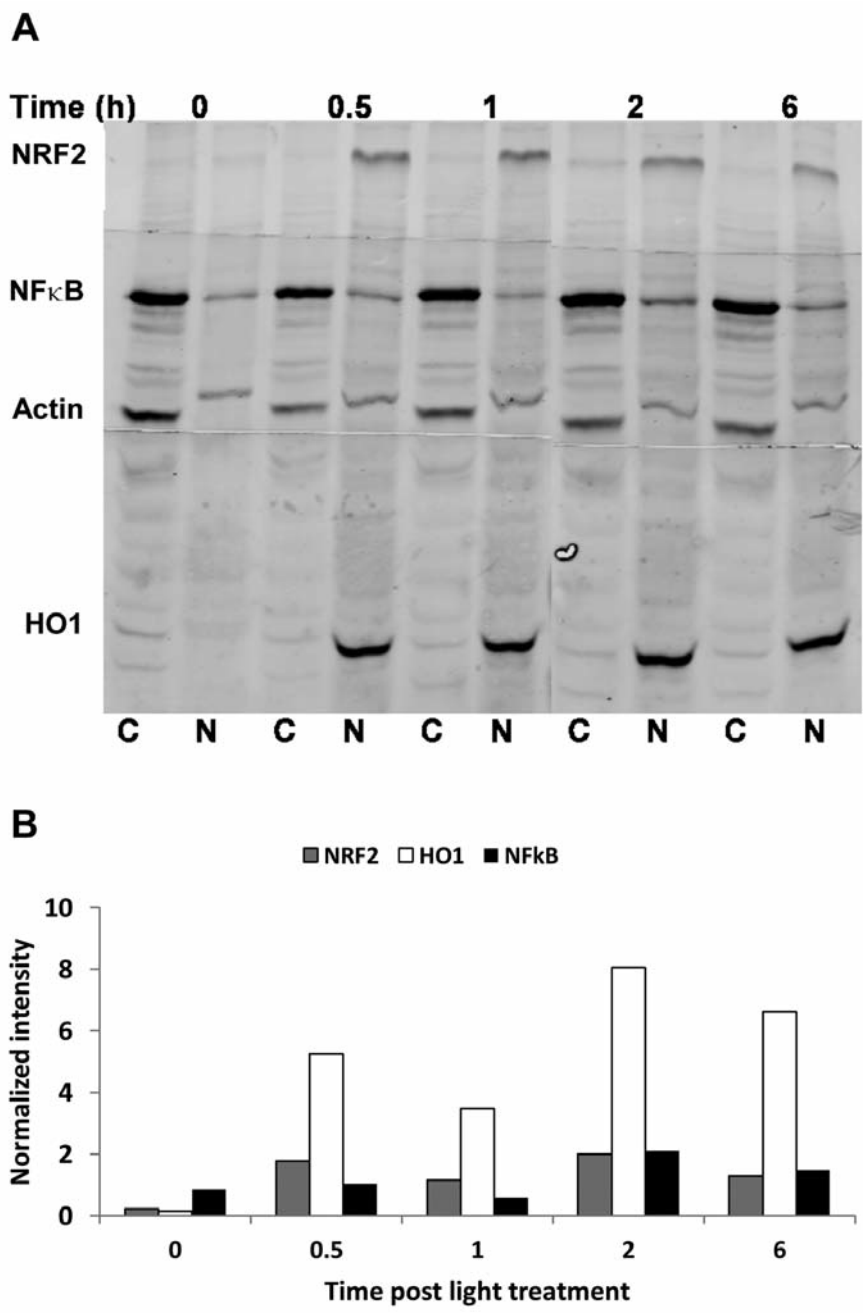

Figure 3. *A: Western blot (representative of three replicate experiments) of A431 cytosolic (C) and nuclear (N) proteins harvested at 0, 0.5, 1, 2, or 6 hours post-light treatment (45 J/cm^2). B: Quantification of band intensity of the nuclear lanes of the blot shown in A, normalized to actin loading controls (Odyssey image analysis).*

western blot of samples collected from a 45 J/cm^2 experiment is shown in Figure 3. NRF2 was essentially undetectable in control samples, but rapidly increased and translocated to the nucleus by 30 min post light treatment at both exposures levels. IR imaging quantification of specific proteins showed that nuclear levels of NRF2 and its downstream target, HO1, were increased significantly (6- and 50-fold, respectively) at 0.5-h post-light treatment, as compared to untreated controls. Both remained elevated throughout the 6-h time course, and increased to higher levels with increased light dose (Figure 3). In contrast, nuclear levels of the redox-sensitive transcription factor NF-κB increased only slightly in response to light treatment (approximately 2-fold) (Figure 3).

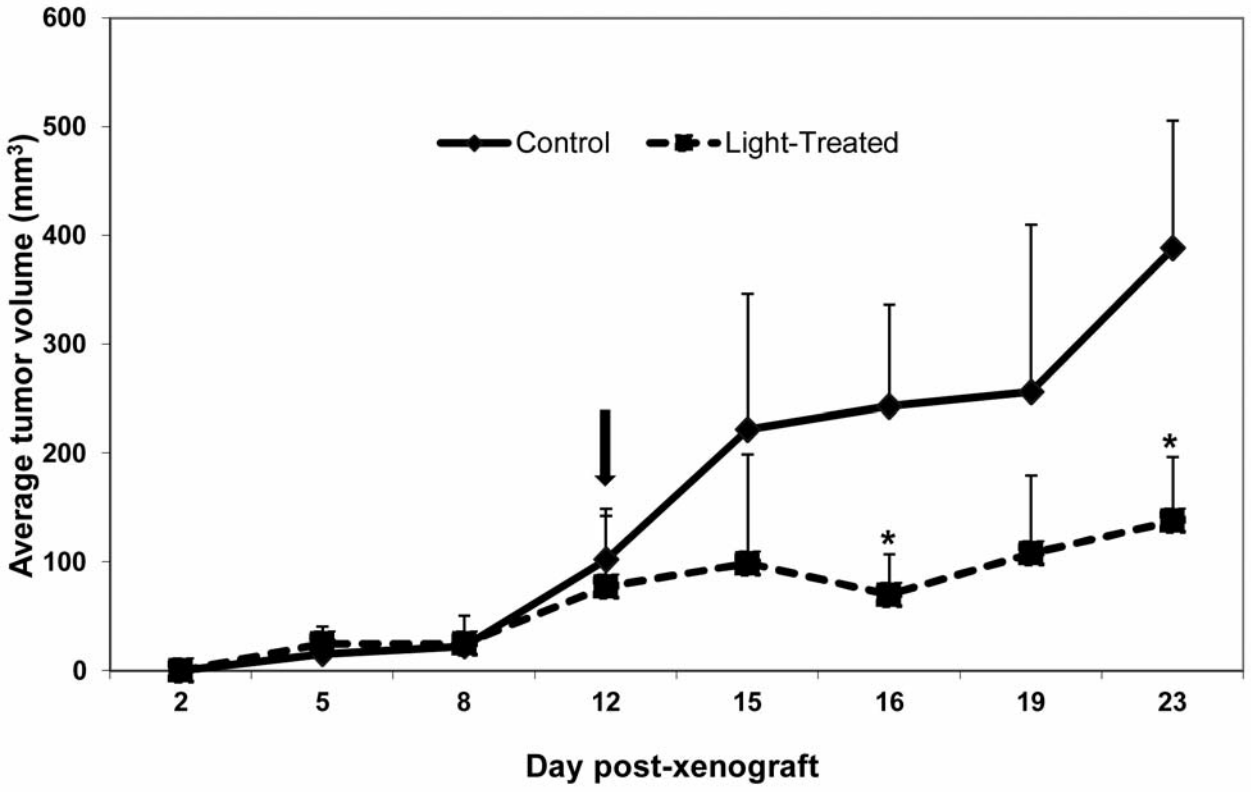

Figure 4. *Growth of human A431 epidermoid tumor xenografts in nude mice. Light treatment began on day 12 (arrow). Error bars indicate one standard deviation (n=10). *Significantly different from untreated controls at each time point (two-sided Student's t-test, p<0.05).*

Growth of human A431 tumor xenografts. Growth of nude mouse A431 xenografts was slowed once light treatment was initiated (Figure 4). Tumor growth was essentially identical in both groups throughout the first 12 days after A431 tumor cell injection. Daily light treatment (90 sec=45 J/cm^2) of half of the tumors was initiated on day 12. Tumor volumes were measured daily and averaged for control and light-treated groups. By four days after initiation of light treatment (day 16), the average volume of the light-treated tumors was significantly lower than that in the untreated controls ($p<0.05$) and was still significantly lower at harvest (day 23) (Figure 4).

Proliferation marker in human A431 tumor xenografts. Harvested tumors were divided evenly and either formalin fixed or flash frozen and solubilized. These tumor samples were then tested for a marker of cell proliferation. PCNA levels were assessed by western blot analysis of flash-frozen tumor samples (Figure 5). Normalized values of quantified PCNA from each sample were added and the mean values of control and light-treated samples were compared. PCNA levels were reduced significantly in light-treated tumors relative to untreated controls, suggesting a decrease in cell proliferation (Figure 5).

Oxidation of proteins was assessed using DNPH-derivatized carbonyls. The level of protein oxidation was assessed in flash-frozen tumor samples using DNPH derivatization of carbonyl groups. Oxidized protein profiles yielded five major oxidized proteins that were selected and relatively quantified in each sample. Overall, protein oxidation was significantly lower in the light-treated samples when compared to controls (Figure 6).

Discussion

A431 cells exposed to blue light exhibited suppressed mitochondrial function as indicated by MTT assay. This effect was dosage dependent and was sustained over the 72-h period after a single 30- or 90-second treatment. Previous studies have reported that long-term exposure to blue light has major effects on mitochondria of retinal ganglia cells and results in cytochrome c release, apoptotic protease activating factor 1 activation and induction of apoptosis (28). Since hemes and flavins absorb blue light most efficiently and many heme-/flavin-containing proteins are concentrated in the inner mitochondrial membrane, it is not surprising that blue light causes changes there. Changes

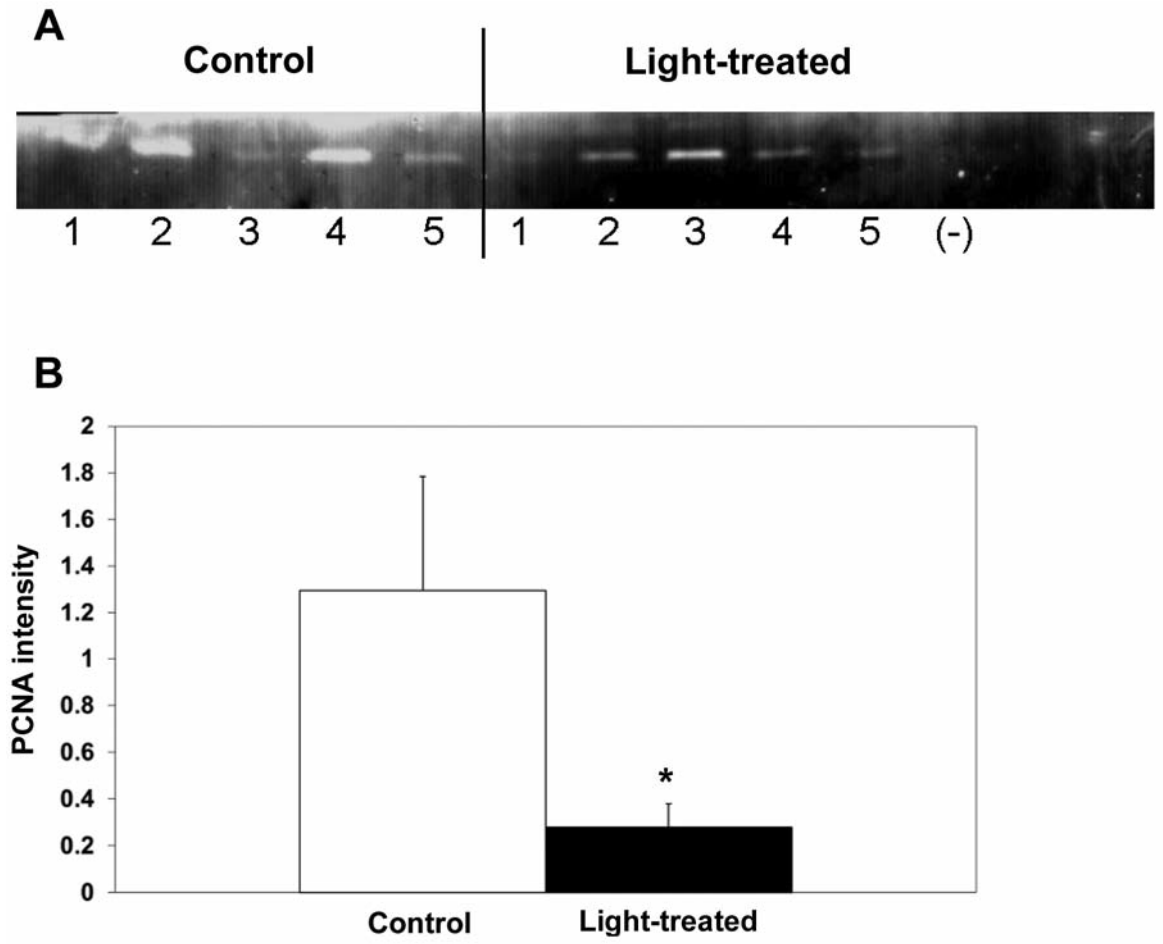

Figure 5. *A: Equal amounts of protein derived from control and light-treated A431 epidermoid tumor xenografts (n=5 mice each) were separated by 9% sodium dodecyl sulfate-polyacrylamide gel electrophoresis, transferred to a polyvinylidene fluoride membrane and exposed to antibody to proliferating cell nuclear antigen (PCNA). B: Quantification of the bands of the blot shown in A (Odyssey image analysis). Data are the means; error bars indicate one standard deviation. *Significantly different from untreated controls (two-sided, Student's t-test, p<0.05).*

in mitochondrial membrane potential would also result in release of ROS that could then activate the phase 2 response. Indeed, we detected rapid accumulation and nuclear translocation of NRF2 and HO1 following light treatment of A431 cells. The very rapid and robust accumulation of nuclear HO1 was surprising. However, there is evidence in other cell models that *HO1* transcripts accumulate and are very rapidly translated in response to stress conditions.

NF-κB is found constitutively in the nucleus of A431 cells, as is often the case for many tumor cell lines. NF-κB target genes such as cyclin D and B-cell lymphoma 2 among others are thought to provide pro-survival/anti-apoptotic contributions to tumorigenicity (29). Importantly, light treatment had relatively little effect on levels of NF-κB in the nucleus, possibly allowing blue light-induced up-regulation of nuclear NRF2 levels and target genes to interfere with NF-κB function and counteract its pro-tumorigenic effects. Many previous studies have looked at the crosstalk between NRF2 and NF-κB signaling pathways to identify areas where NRF2 signaling has as an anti-inflammatory effect. Whereas these studies have not yet provided definitive evidence of direct NRF2–NF-κB interactions, some have shown that NRF2 competes with NF-κB for co-activator proteins such as p300 histone deacetylase (30), and thus may influence activator efficiency indirectly.

Heme oxygenase is a major enzyme in heme metabolism and produces breakdown products of biliverdin, iron, and carbon monoxide. Carbon monoxide signaling has also become a topic of much interest in recent years and may play a role in the anti-inflammatory properties of HO1, as well as in protection against photocarcinogenesis in response to UVB exposure (31). In addition, heme oxygenase has been reported to translocate to the nucleus and act as a

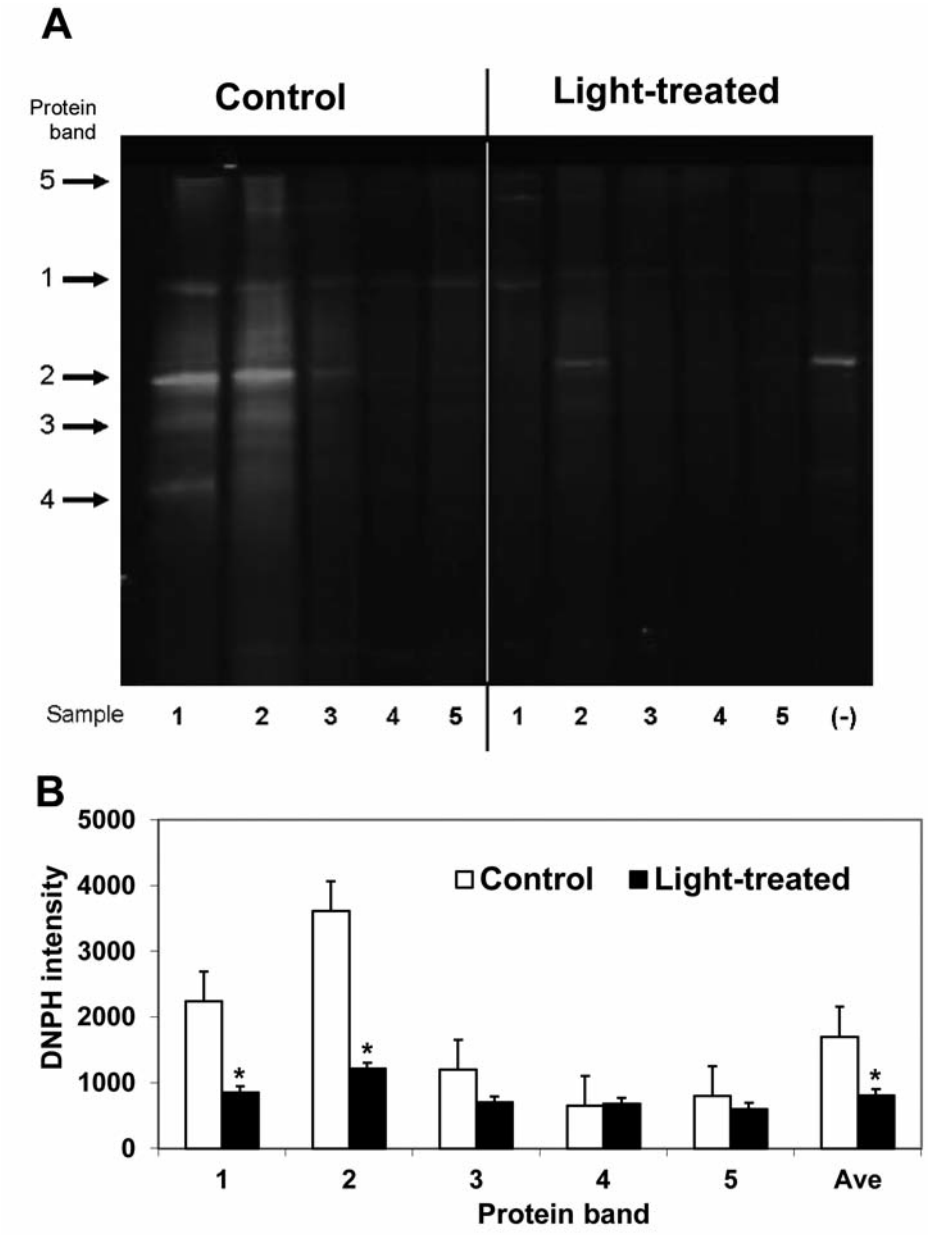

Figure 6. *Protein oxidation analysis via dinitrophenylhydrazine (DNPH)-derivatized carbonyls (OxyBlot). A: Representative immunoblot of equal amounts of DNPH-derivatized protein from tumor lysates separated by 12% sodium dodecyl sulfate-polyacrylamide gel electrophoresis. Proteins containing oxidized carbonyl groups were identified via antibody to DNPH and quantified via Odyssey scanning and analysis. Arrows indicate 5 specific bands used for quantitation analysis. The negative control (−) was tissue lysate from normal mouse skin. B: Scanning results of each sample, with the means of all groups in the far right set of columns. Error bars indicate one standard deviation (n=5). *Significantly different from untreated controls (two-sided Student's t-test, p<0.05).*

transcriptional repressor of NF-κB-regulated target genes (32) and may support NRF2-mediated anti-inflammatory and anti-tumorigenic effects in this way.

Analysis of A431 xenografts showed that growth of light-treated tumors slowed significantly. Evaluation of the PCNA levels of control and light-treated tumors suggests a general suppression of proliferation in response to blue light treatment. Oxidation levels in light-treated tumors were decreased overall, as would be expected with up-regulation of the phase 2 antioxidant response. Reduction in ROS in the light-treated tumors may serve to reduce the pro-proliferative effects of oxidative stress (33).

In conclusion, this study showed that blue light activates the phase 2 response in cultured epidermoid carcinoma cells and reduces their viability in a dose-dependent fashion. This effect translated to an *in vivo* xenograft model that showed decreased tumor cell growth, proliferation, and oxidation levels in light-treated tumors. These results suggest that cellular responses to these light energies is worth further study and may provide future therapeutic interventions for inflammation and cancer.

References

1 Aggarwal BB, Quintanilha AT, Cammack R and Packer L: Damage to mitochondrial electron transport and energy coupling by visible light. Biochem Biophys Acta *502*: 367-382, 1978.

2 Gorgidze LA, Oshemmkova SA and Vorobjev IA: Blue light inhibits mitosis in tissue culture cells. Biosci Rep *18(4)*: 215-224, 1998.

3 Pflaum M, Kielbassa C, Garmyn M and Epe B: Oxidative DNA damage induced by visible light in mammalian cells: extent, inhibition by antioxidants, and genotoxic effect. Mutation Res *408*: 137-146, 1998.

4 Beatty S, Koh HH, Henson D and Boulton M: The role of oxidative stress in the pathogenesis of age-related macular degeneration. Surv Opthamol *45(2)*: 115-134, 2000.

5 Winkler BS, Boulton ME, Bottsch JD and Sternberg P: Oxidative damage and age-related macular degeneration. Mol Vis *5*: 32, 1999.

6 Zhong J, Edwards G, Raval C, Haibin L and Tyrrell RM: The role of Nrf2 in ultraviolet A mediated heme oxygenase 1 induction in human skin fibroblasts. Photoch Photobio Sci *9*: 18-24, 2010.

7 Cullinan SB, Gordan JD, Jin J, Harper JW and Diehl JA: The Keap1-BTB protein is an adaptor that bridges Nrf2 to a Cul3-based E3 ligase: oxidative stress sensing by a Cul3-Keap1 ligase. Mol Cell Biol *24*: 8477-8486, 2004.

8 Furukawa M and Xiong Y: BTB protein Keap1 targets antioxidant transcription factor Nrf2 for ubiquitination by the Cullin3-Roc1 ligase. Mol Cell Biol *25*: 162-171, 2005.

9 Kobayashi A, Kang MI, Okawa H, Ohtsuji M, Zenke Y, Chiba T, Iqarashi K and Yamamoto M: Oxidative stress sensor Keap1 functions as an adaptor for Cul3-based E3 ligase to regulate proteasomal degradation of Nrf2. Mol Cell Biol *24*: 7130-7139, 2004.

10 Motohashi H and Yamamoto M: Nrf2-Keap1 defines a physiologically important stress response mechanism. Trends Mol Med *10*: 549-557, 2004.

11 Padmanabhan B, Tong KI, Ohta T, Nakamura Y, Scharlock M, Ohtsuji M, Kang MI, Kobayashi A, Yokoyama S and Yamamoto M: Structural basis for defects of Keap 1 activity provoked by its point mutations in lung cancer. Mol Cell *21*: 689-700, 2006.

12 Li W, Khor TO, Xu C, Shen G, Jeong W-S, Yu S and Kong A-N: Activation of Nrf-2-antioxidant signaling attenuates NFκB-inflammatory response and elicits apoptosis. Biochem Pharmacol *76*: 1485-1489, 2008.

13 Itoh K, Chiba T, Takahashi S, Ishii T, Igarashi K, Katoh Y, Oyake T, Hayashi N, Satoh K, Hatayama I, Yamamoto M and Nabeshima Y: An Nrf2/small Maf heterodimer mediates the induction of phase II detoxifying enzyme genes through antioxidant response elements. Biochem Bioph Res Co *236*: 313-322, 1997.

14 Ishii T, Itoh K, Takahashi S, Sato H, Yanagawa T, Katoh Y, Bannai S and Yamamoto M: Transcription factor Nrf2 coordinately regulates a group of oxidative stress-inducible genes in macrophages. J Biol Chem *275(21)*: 16023-16029, 2000.

15 Ito T, Kimura S, Seto K, Warabi E, Kawachi Y, Shoda J, Tabuchi K, Yamagata K, Hasegawa S, Bukawa H, Ishii T and Yanagawa T: Peroxiredoxin I plays a protective role against UVA irradiation through reduction of oxidative stress. J Dermatol Sci *74*: 9-17, 2014.

16 Khor TO, Huang MT, Dwon KH, Chan JY, Reddy BS and Kong AN: Nrf2-deficient mice have an increased susceptibility to dextran sulfate sodium-induced colitis. Cancer Res *66*: 11580-11584, 2006.

17 Thimmulappa RK, Lee H,Rangasamy T, Reddy SP, Yamamoto M, Kensler TW and Biswal S: Nrf2 is a critical regulator of the innate immune response and survival during experimental sepsis. J Clin Invest *116(4)*: 984-995, 2006.

18 Khor TO, Keum YS, Lin W, Kim JH, HuR, Shen G, Xu C, Gopalakrishnan A, Reddy B, Zheng X, Conney AH and Kong AN: Combined inhibitory effects of curcumin and phenethyl isothiocyanate on the growth of human PC-3 prostate xenografts in immunodeficient mice. Cancer Res *66*: 613-621, 2006.

19 Xu C, Huang MT, Shen G, Yuan X, Lin W, Khor TO, Conney AH and Kong AN: Inhibition of 7,12-dimethylbenz(a) anthracene-induced skin tumorigenesis in C57BL/6 mice by sulforaphane is mediated by nuclear factor E2-related factor 2. Cancer Res *66*: 8293-6, 2006.

20 Kundu JK, Na HK, Chun KS Kim YK, Lee SJ, Lee SS, Lee OS, Sim YC and Surh YJ: Inhibition of phorbol ester-induced COX-2 expression by epigallocatechin gallate in mouse skin and cultured human mammary epithelial cells. J Nutr 133: 3805S-3810S, 2003.

21 Kundu JK, Shin YK, Kim SH and Surh YJ: Resveratrol inhibits phorbol ester-induced expression of Cox-2 and activation of NFκB in mouse skin by blocking IκB kinase activity. Carcinogenesis *27*: 1465-1474, 2006.

22 Myzak MC and Dashwood RH: Chemoprotection by sulforaphane: keep one eye beyond Keap1. Cancer Lett *233*: 208-218, 2006.

23 Surh Y-J and Na H-K: NF-κB and NRF2 as prime molecular targets for chemoprevention and cytoprotection with anti-inflammatory and antioxidant phytochemicals. Genes Nutr 2: 313-317, 2008.

24 Heiss E and Gerhauser C: Time-dependent modulation of thioredoxin reductase activity might contribute to sulforaphane mediated inhibition of NF-κB binding to DNA. Antioxid Redox Sign *7*: 1601-1611, 2005.

25 Heiss E, Herhaus C, Klimo K, Bartsch H and Gerhauser C: Nuclear factor κB is a molecular target for sulforaphane-mediated anti-inflammatory mechanisms. J Biol Chem *276*: 32008-32015, 2001.

26 Lewis J, Wataha JC, Messer RLW, Hsu SD, Yamamoto T and Caughman G: Blue light differentially alters cellular redox properties. J Biomed Mater Res *72(2)*: 223-229, 2005.

27 Frankenberger M, Pforte A, Sterndorf T, Passlick B, Baeurle PA and Ziegler-Heitbrock HWL: Constitutive nuclear NF-κB in cells of the monocyte lineage. Biochem J *304*: 87-94, 1994.

28 Huang C, Zhang P, Wang W, Xu Y, Wang M, Chen X and Dong X: Long-term blue light exposure induces RGC-5 cell death *in vitro*: involvement of mitochondria-dependent apoptosis, oxidative stress, and MAPK signaling pathways. Apoptosis *19(6)*: 922-32, 2014.

29 Del Prete A, Allavena P, Santoro G, Fumarulo R, Corsi MM and Mantovani A: Molecular pathways in cancer-related inflammation. Biochem Medica *21(3)*: 264-275, 2011.
30 Kim S-W, Lee H-K, Shin J-H and Lee J-K: Up-down regulation of HO1 and iNOS gene expressions by ethyl pyruvate *via* recruiting p300 to NRF2 and depriving it from p65. Free Radical Bio Med *65*: 468-476, 2013.
31 Allanson M and Reeve VE: Carbon monoxide signaling reduces photocarcinogenesis in the hairless mouse. Cancer Immunol Immun *56*: 1807-1815, 2007.
32 Lin Q, Weis S, Yang G, Weng Y-H, Helston R, Rish K, Smith A, Bordner J, Polte T, Guanitz F and Dennery PA: Heme oxygenase-1 protein localizes to the nucleus and activates transcription factors important in oxidative stress. J Biol Chem *282*: 20621-20633, 2007.
33 Groeger G, Quiney C and Cotter TG: Hydrogen peroxide as a cell-survival signaling molecule. Anitoxid Redox Signal *11(11)*: 2655-2671, 2009.

Received June 18, 2014
Revised August 5, 2014
Accepted August 5, 2014